hsa_circ_0000523/miR-let-7b/METTL3 axis regulates proliferation, apoptosis and metastasis in the HCT116 human colorectal cancer cell line

YANSHENG WANG[1], BAOLEI ZHANG[2], YUN ZHU[3], YONG ZHANG[1], LI LI[1], TAO SHEN[4], HAO LIU[1] and YIRONG TENG[5]

[1]Department of General Surgery, The 6th Affiliated Hospital of Kunming Medical University, The People's Hospital of Yuxi City, Yuxi, Yunnan 653100; [2]Department of Gastrointestinal Surgery, Liaocheng People's Hospital Affiliated to Shandong University and Clinical School of Taishan Medical University, Liaocheng, Shandong 271099; [3]Department of Health Screening Center, The 6th Affiliated Hospital of Kunming Medical University, The People's Hospital of Yuxi City, Yuxi, Yunnan 653100; [4]Department of Colorectal Surgery, The Third Affiliated Hospital of Kunming Medical University, Kunming, Yunnan 650118; [5]Department of General Practice, The 6th Affiliated Hospital of Kunming Medical University, The People's Hospital of Yuxi City, Yuxi, Yunnan 653100, P.R. China

Received June 4, 2021; Accepted February 24, 2022

DOI: 10.3892/ol.2022.13306

Abstract. Circular RNAs (circRNAs/circs) have gained attention as a class of potential biomarkers for the early detection of multiple cancers. However, the functions and mechanisms of circRNAs in the oncogenesis of human colorectal cancer (CRC) remain to be elucidated. The present study aimed to investigate the roles of *hsa_circ_0000523* and its parental gene methyltransferase-like 3 (*METTL3*) in regulating cell proliferation, apoptosis and invasion in the HCT116 human CRC cell line. To uncover the regulated function of *hsa_circ_0000523* in HCT116 cells, a dual-luciferase reporter assay, flow cytometry, reverse transcription-quantitative PCR, Cell Counting Kit-8 assay, cell invasion and western blot assay were used. In HCT116 cells, *hsa_circ_0000523* indirectly regulated *METTL3* expression by suppressing the transcription of microRNA (*miR*)-*let-7b*. The expression of *METTL3* promoted cell proliferation and suppressed apoptosis. In the present study, it was found that *miR-let-7b* promoted cell viability and inhibited apoptosis and invasion, while *circ_0000523* exerted the opposite effects. Higher levels of *METTL3* expression were associated with more aggressive tumor invasion. The present results suggest that circRNAs and *METTL3* may be applied for highly sensitive diagnosis of CRC and for predicting prognosis in patients who have undergone therapy.

Correspondence to: Dr Hao Liu, Department of General Surgery, The 6th Affiliated Hospital of Kunming Medical University, The People's Hospital of Yuxi City, 21 Nieer Road, Yuxi, Yunnan 653100, P.R. China
E-mail: handy_lau712@163.com

Dr Yirong Teng, Department of General Practice, The 6th Affiliated Hospital of Kunming Medical University, The People's Hospital of Yuxi City, 21 Nieer Road, Yuxi, Yunnan 653100, P.R. China
E-mail: tengyirong1836@163.com

Key words: *hsa_circ_0000523*, methyltransferase-like 3, colorectal cancer, HCT116

Introduction

Colorectal cancer (CRC) is one of the most common malignancies worldwide (1,2). More than 1 million new cases of CRC were diagnosed worldwide in 2012, which accounts for ~10% of the global cancer burden (3). Currently, CRC is the fourth most common cause of cancer-related mortality (4,5). Although conventional treatments such as surgery, chemotherapy, radiotherapy and immunotherapy have improved the survival of patients with CRC, the mortality and relapse rates remain high (5,6). Therefore, more specific mechanism-based treatments are greatly needed.

Circular RNAs (circRNAs/circs) have gained attention as a class of potential biomarkers for the early detection of CRC (7). circRNA is a newly discovered type of non-coding RNA, which is distinct from the traditional linear RNA that has 5'- and 3'-ends (8). circRNAs are formed by exon skipping or back-splicing events, during which the 5'-end of an upstream exon is spliced together with the 3'-end of the downstream exon to form a circular molecule of RNA (8,9). circRNAs have been demonstrated to serve an important role in post-transcriptional regulation by acting as microRNA (miRNA/miR) sponges to competitively inhibit RNA/miRNA transcriptional regulation (10,11).

The abnormal expression of circRNA is closely associated with various diseases, including CRC (12-14). Jiang *et al* (15)

identified a large set of differentially expressed circRNAs in a primary CRC cell line (SW480) and a metastatic CRC cell line (SW620), relative to a normal colon cell line (NCM460). *hsa_circ_000984* has been reported to promote colon cancer growth and metastasis by sponging miR-106b (16). Furthermore, Bachmayr-Heyda *et al* (17) demonstrated a global reduction in circRNA abundance in CRC cell lines and clinical CRC specimens compared with normal tissues. The authors described five specific circRNAs (circ0817, circ3203, circ6229, circ7374 and circ7780) and proposed a potentially negative association between global circRNA abundance and cell proliferation.

Among the five circRNAs identified, the present study focused on circ6229 (also known as *circ_0000523*) and its corresponding gene/linear mRNA, methyltransferase-like 3 (*METTL3*). As a major RNA N6-adenosine methyltransferase, *METTL3* is widely implicated in mRNA biogenesis, decay and translation control (18). *METTL3* has previously been demonstrated to promote the growth, survival and invasion of numerous human cancers (19), such as lung cancer (20), hepatocellular carcinoma (21), breast cancer (22) and pancreatic cancer (23). However, the precise role of *METTL3* in the tumorigenesis and pathogenesis of CRC remains largely unknown.

HCT116 cells are a population of malignant cells that were isolated from the primary cell culture of a single human colonic carcinoma (24). In present study, the regulatory role of *hsa_circ_0000523* in HCT116 cells was explored in detail. Dual-luciferase reporter assay, reverse transcription-quantitative PCR (RT-qPCR) and some rescue experiments were applied to confirm the existence of the *hsa_circ_0000523/miR-let-7b/METTL3* axis. FCM was used to count the apoptotic cells. Cell Counting Kit-8 (CCK-8) and invasion assays were performed to monitor the activities of the HCT116 cells. The present study suggests a potential role for the *hsa_circ_0000523/miR-let-7b/METTL3* axis in the tumorigenesis and pathogenesis of human CRC.

Materials and methods

Cell culture. The HCT116 human CRC cell line (cat. no. CCL-247) was obtained from American Type Culture Collection. Cells were maintained in DMEM (Thermo Fisher Scientific, Inc.) supplemented with 10% FBS (Thermo Fisher Scientific, Inc.), 100 units/ml penicillin and 100 μg/ml streptomycin (Thermo Fisher Scientific, Inc.). Cells were grown in a humidified atmosphere with 5% CO_2 at 37˚C. Cells were cultured in 75-cm^2 flasks or 10-cm plates (Corning, Inc.), with the confluence maintained below 80%. After digestion with 0.25% (w/v) trypsin and 0.5 mM EDTA (Thermo Fisher Scientific, Inc.), cells were passaged every 2-3 days with a subcultivation ratio between 1:3 and 1:8.

Plasmid constructs and small interfering RNA (siRNA) oligos. Total RNA was extracted from the HCT116 cells using TRIzol® reagent (Thermo Fisher Scientific, Inc.) and further purified with two phenol-chloroform treatments, and then treated with RQ1 DNase (Promega Corporation) to digest DNA. The quality and quantity of the purified RNAs were measured by a Nano Photometer spectrometer with the absorbance at 260/280 nm. The mixture was verified by 1.2% agarose gel electrophoresis. The cDNA was synthesized with random primers with the High-capacity cDNA Reverse-Transcription Kit (Takara Biotechnology Co., Ltd.) according to the manufacturer's instructions. The full-length cDNA for human *METTL3* (GenBank accession no. NM_019852.5) was obtained from the cDNA library of HCT116 cells by PCR, using the following protocol: 98˚C for 10 min, followed by 98˚C for 10 sec, 55˚C for 5 sec and 72˚C for 2 min for 35 cycles, and then 72˚C for 10 min. The primers are listed in Table I. The vector used to generate full-length wild-type (WT) *METTL3* and *hsa_circ_0000523* was mammalian expression vector pcDNA3.1 (Thermo Fisher Scientific, Inc.). The *METTL3* coding sequence or *circ_0000523* fragment was subcloned into the pcDNA3.1 vector via *Kpn*I and *Bam*HI double-enzymatic sites. Positive clones were selected, and the plasmid expressing *METTL3* or *hsa_circ_0000523* was verified by sequencing. The siRNA oligos used in the present study were designed and synthesized by Wuhan GeneCreate Biological Engineering Co., Ltd. The sequences for these siRNA oligos were as follows: Negative control siRNA oligo (*METTL3*-con) sense, 5'-GCUACUUCAGACGAGCAUUdT dT-3'; *METTL3*-specific siRNA oligo (*METTL3*-si) sense, 5'-GCUGCACUUCAGACGAAUUdTdT-3'; negative control oligo for *hsa_circ_0000523* (circ-con) sense, 5'-CAACAG AGCAAGAAGUAGAUdTdT-3'; and *circ_0000523*-specific siRNA oligo (circ-si) sense, 5'-CAACAGAGCAAGAAGAUC UAdTdT-3'.

Transfection of plasmids and siRNA oligos. HCT116 cells were transfected with the empty pcDNA3.1 vector (*METTL3*-EV), *METTL3*-expressing pcDNA3.1 vector (*METTL3-OE*), *METTL3*-con, *METTL3-si*, circ-EV, circ-OE, circ-con, circ-si, mimics, mimics NC, inhibitor and inhibitor NC using Lipofectamine® 2000 reagent (Thermo Fisher Scientific, Inc.) according to the manufacturer's protocol. miR-let-7b mimic sense (5'-UGAGGUAGUAGGUUGUGUGGUU-3'), its negative control (5'-UCACAACCUCCUAGAAAGAGUAGA-3'), inhibitor (5'-AACCACACAACCUACUACCUCA-3') and inhibitor NC (5'-UCUACUCUUUCUAGGAGGUUG UGA-3') were synthesized by Wuhan GeneCreate Biological Engineering Company. The RNA concentrations of mimics and inhibitor were 0.32 and 0.26 μg/μl, respectively. HCT116 cells ($1x10^4$) were seeded in 6-well plates and maintained at a confluence of 70-80% in complete culture medium. Then, 2.5 μg plasmid or 100 pmol siRNA oligo was added to 250 μl Opti-MEM (Thermo Fisher Scientific, Inc.), and 5 μl Lipofectamine 2000 reagent was added to 250 μl Opti-MEM. The diluted plasmid or siRNA oligo was mixed with diluted Lipofectamine 2000 reagent and kept at room temperature for 20 min. After 500 μl serum-free medium was added to each well, the Opti-MEM mixture was added. After transfected cells were incubated at 37˚C for 4 h, the culture medium was changed to regular DMEM supplemented with 10% FBS. After 48 h, the subsequent experiments were performed.

RNA isolation and reverse transcription. Total RNA was extracted from cells using TRIzol reagent (Thermo Fisher Scientific, Inc.) according to the manufacturer's protocols. Briefly, after treatment, cell pellets were resuspended in

Table I. Sequences of primers used for reverse transcription-quantitative PCR in the present study.

Gene	Primer sequence (5'-3')
hsa_circ-0000523	F: CAGCATCGGAACCAGCAAAG
	R: CTGGGCTGTCACTACGGAAG
miR-let-7b	F: GGGTGAGGTAGTAGGTTGT
	R: CAGTGCGTGTCGTGGAGT
U6	F: CTCGCTTCGGCAGCACA
	R: AACGCTTCACGAATTTGCGT
METTL3	F: GTGTCGGAGGTGATTCCAGT
	R: CTGCGCATCTCATCATCTGT
GAPDH	F: GTCAGTGGTGGACCTGACCT
	R: TGCTGTAGCCAAATTCGTTG

F, forward; R, reverse; circ, circular RNA; miR, microRNA; *METTL3*, methyltransferase-like 3.

1 ml TRIzol and mixed well. Then, 0.2 ml chloroform was added to the cell suspension, which was shaken vigorously for 15 sec and then incubated for 3 min at room temperature. After centrifugation of the suspension at 12,000 x g for 10 min at 4˚C, supernatant was collected and subjected to RNA precipitation by adding 0.5 ml isopropanol at 4˚C. The RNA pellet was obtained by centrifugation at 12,000 x g for 10 min at 4˚C, and then washed with 75% ethanol. The appropriate amount of RNase-free distilled water was used to dissolve extracted RNA. The concentration of RNA was measured with a NanoDrop 2000 Spectrophotometer (Thermo Fisher Scientific, Inc.). For each sample, 1 μg RNA was reverse transcribed into cDNA using the ReverTra Ace qPCR RT Kit (cat. no. FSQ-101; Toyobo Life Science) according to the specifications in the product manual.

RT-qPCR. For RT-qPCR, SYBR Green Realtime PCR Master Mix (cat. no. QPK-212; Toyobo Life Science) was used to measure the expression of targeted genes according to the manufacturer's protocol. For quantification of *hsa_circ_0000523* and *let-7b*, *U6* was used as an internal reference gene. *GAPDH* was used as an internal reference gene for the quantification of *METTL3*. The conditions for PCR were set as follows: Pre-denaturation at 95˚C for 1 min, followed by 40 cycles of denaturation at 95˚C for 15 sec, and annealing and elongation at 60˚C for 30 sec. The 7900HT Real-Time PCR System (Applied Biosystems; Thermo Fisher Scientific, Inc.) was used to perform the assay. The $2^{-\Delta\Delta Cq}$ method was used to calculate differences in target gene expression between the experimental and control groups. The calculation formula was as follows: $\Delta\Delta Cq=\Delta Cq_{experimentalgroup}-\Delta Cq_{normalgroup}$, $\Delta Cq=Cq_{targetgene}-Cq_{internalreference}$ (25). The sequences of primers used for RT-qPCR are presented in Table I.

Western blot (WB) assay. HCT116 human CRC cells with various treatments were washed twice using PBS buffer. Total protein was extracted from the treated cells using NE-PER Nuclear and Cytoplasmic Extraction Reagents (Thermo Fisher Scientific, Inc.) according to the manufacturer's protocols and then measured using a BCA assay. Briefly, the tube was vigorously vortexed for 15 sec. Then, ice-cold cytoplasmic extraction reagent II was added to the tube and the tube was vortexed for another 5 sec. The tube was centrifuged at 16,000 x g for 5 min at 4˚C, and then the supernatant was collected. The insoluble (pellet) fraction was suspended in ice-cold nuclear extraction reagent. Subsequently, the collected fraction was vortexed for 15 sec and the tube was centrifuged at 16,000 x g (15 min, 4˚C). Lastly, the supernatant fraction was transferred to a clean tube and stored at -80˚C until use. Proteins were quantified by the BCA method. The proteins (50 μg) were separated on 12% gels using SDS-PAGE (Beyotime Institute of Biotechnology), and then quickly transferred onto a PVDF membrane.. The membrane was blocked with 5% skimmed milk for 45 min at 37˚C, and then probed with primary antibodies for 12 h at 4˚C. The membrane was washed three times and probed with the secondary antibodies for 1 h at 25˚C. The signal was detected using an ECL system (MilliporeSigma) and the gray level was assessed using ImageJ 1.8.0 software (National Institutes of Health). The primary antibodies were: Anti-*METTL3* antibody (EPR18810; 1:2,000 dilution; cat. no. ab195352; Abcam) and GAPDH monoclonal Antibody (1:10,000 dilution; catalog no. 60004-1-Ig; ProteinTech Group, Inc.). The secondary antibody was HRP-conjugated Affinipure Goat Anti-Rabbit IgG(H+L) (1:10,000 dilution; catalog no. SA00001-2; ProteinTech Group, Inc.). All antibodies used in the WB assay were diluted in 5% skimmed milk powder.

Dual-luciferase reporter assay. The binding sites among *miR-let-7b*, *circ_0000523* and *METTL3* were predicted by Bielefeld Bioinformatics Service online software (https://bibiserv.cebitec.uni-bielefeld.de/prevres.jsf). The WT *miR-let-7b* along with the 3'-UTR of *METTL3* that contained the predicted *miR-let-7b* binding site or a sequence with mutations (MUT) were amplified and inserted into the pmirGLO vector (Promega Corporation), resulting in the WT luciferase reporter construct. The vectors (*miR-let-7b*-WT, *miR-let-7b*-MUT, *METTL3*-WT or *METTL3*-MUT), *miR-let-7b* mimics and negative control mimics, which were synthesized by Wuhan GeneCreate Biological Engineering Company, were transfected into CRC cells using Lipofectamine 3000 (Thermo Fisher Scientific, Inc.). After 48 h, the luciferase activity was measured using a luciferase reporter system (Promega Corporation), with *Renilla* luciferase activity as an internal control. The sequences of mimics *miR-let-7b* and mimics NC were as follows: *miR-let-7b* mimic sense, 5'-UGAGGUAGUAGGUUGUGUGGUU-3'; NC sense, 5'-UCACAACCUCCUAGAAAGAGUAGA-3'.

CCK-8 assay to measure cell proliferation. After transfection of empty pcDNA3.1 vector, *METTL3*-expressing pcDNA3.1 vector, *METTL3*-con oligo or *METTL3*-si oligo, HCT116 cells were seeded into flat-bottomed 96-well plates at a density of $3x10^3$-$6x10^3$ cells per well in 100 μl culture medium. Each treatment condition was replicated in nine wells. Cells were incubated for 24, 48 or 72 h in an incubator with 5% CO_2 at 37˚C. Cell proliferation was analyzed with a CCK-8 assay (Beyotime Institute of Biotechnology) according to the manufacturer's protocol. Briefly, 20 μl CCK-8 reagent (5 mg/ml)

was added to the culture medium, and cells were cultured for an additional 4 h. The optical density values of all wells were measured with a plate reader (Thermo Fisher Scientific, Inc.) at 450 nm.

Cell apoptosis. HCT116 cells seeded in 6-well plates were transfected with empty pcDNA3.1 vector, *METTL3*-expressing pcDNA3.1 vector, *METTL3*-con oligo or *METTL3*-si oligo, as aforementioned. At 48 h after transfection, cells were detached by incubation with 0.25% trypsin-EDTA solution (Thermo Fisher Scientific, Inc.) and were harvested. Flow cytometry analysis was performed to detect apoptosis using the Annexin V-FITC/PI apoptosis kit (Beyotime Institute of Biotechnology) according to the manufacturer's protocol. Briefly, after one wash in PBS and one wash in binding buffer, cells were stained with Annexin V-FITC/PI for 20 min at room temperature in the dark. After another wash in binding buffer, labelled cells were detected immediately using a flow cytometer (CytoFLEX S; Beckman Coulter, Inc.). Data were analyzed with CytExpert 2.0 Software (Beckman Coulter, Inc.).

Cell invasion. The cellular potential for invasion was determined using a 24-well Transwell plate with 8.0-μm Pore Polyester Membrane Inserts (Corning, Inc.). Matrigel (Corning, Inc.) was melted overnight at 4˚C and diluted to a final concentration of 1 mg/ml in pre-cooled serum-free medium. Then, 100 μl diluted Matrigel was added to the bottom of the upper chamber. The plate was then incubated at 37˚C for 4-5 h to dry the Matrigel. At 24 h after transfection, HCT116 cells in the logarithmic growth phase were seeded in triplicate at a density of $1x10^6$ cells/chamber. Cells were seeded on top of the Transwell plate in 100 μl DMEM supplemented with 0.1% bovine serum albumin (Thermo Fisher Scientific, Inc.). Then, 0.8 ml DMEM supplemented with 10% FBS (Thermo Fisher Scientific, Inc.) was added to the lower chamber as a chemoattractant. After 24 h of incubation at 37˚C, cells on the top surface of the insert were removed with a cotton swab. Cells that had invaded the lower surface of the membrane were fixed with 4% paraformaldehyde at 37˚C for 15 min and stained with 800 μl Giemsa solution at 37˚C for 20 min (Beyotime Institute of Biotechnology). Cells were visualized using a light microscope (CKX-41; Olympus Corporation). Cell counts were obtained from three randomly selected optical fields.

Statistical analysis. All data were analyzed using SPSS Version 21.0 software (IBM Corp.). All values are presented as the mean ± SD. Three independent experiments were performed Quantitative data were compared using the χ^2 test. For only two comparisons, statistically significant differences between means were determined using an unpaired Student's t-test. For multiple comparisons, the significance was identified by simple one-way ANOVA followed by a Tukey's post-hoc test. $P<0.05$ was considered to indicate a statistically significant difference.

Results

hsa_circ_0000523 regulates METTL3 expression by modulating levels of miR-let-7b in HCT116 cells. To explore the role of *hsa_circ_0000523* circRNA in the tumorigenesis and pathogenesis of CRC, an *in vitro* model was established by manipulating the expression of *hsa_circ_0000523* in the HCT116 human CRC cell line. As shown in Fig. 1A, the mRNA expression levels of *circ_0000523* were successfully increased more than 20-fold in the circ overexpression (circ-OE) group compared with cells transfected with empty vector (circ-EV). Next, this circRNA was knocked down in HCT116 cells. Efficient knockdown of *hsa_circ_0000523* was observed in HCT116 cells transfected with *hsa_circ_0000523*-specific siRNA oligo (circ-si), in which *hsa_circ_0000523* expression was 80% less than that in HCT116 cells transfected with control siRNA oligo (circ-con) (Fig. 1A). Next, the effect of *hsa_circ_0000523* expression on *METTL3* and *miR-let-7b*, a microRNA that may be a target of *hsa_circ_0000523*, was evaluated in HCT116 cells. A negative association between the expression of *hsa_circ_0000523* and *miR-let-7b* was observed (Fig. 1B). Among the various treatment conditions, HCT116 cells transfected with *hsa_circ_0000523*-expressing plasmid (circ-OE) displayed the highest level of *hsa_circ_0000523* expression and the lowest level of *miR-let-7b* expression.

Among all treatment groups, the circ-si group had the highest expression of *miR-let-7b* (Fig. 1B). Expression of *METTL3*, one of the targets of *miR-let-7b*, was upregulated in circ-OE group, while knockdown of *hsa_circ_0000523* exerted an inhibitory effect (Fig. 1C). Next, the regulatory effect of *miR-let-7b* on *METTL3* was verified. A mimic and an inhibitor of *miR-let-7b* were synthesized and then transfected into HCT116 cells. The transfection efficiency was validated by RT-qPCR (Fig. 1D). The reduction of *METTL3* was not significant in miR-treated cells, but the miRNA inhibitor increased the protein level of *METTL3* (Fig. 1E). The binding sequence of *miR-let-7b* in the 3'UTR of *METTL3* mRNA and *circ_0000523* that was predicted by BiBiserv prediction software is shown in Fig. 1F. Lastly, a luciferase reporter assay was implemented to verify the regulatory effect of *miR-let-7b* on *METTL3*. As shown in Fig. 1G, luciferase activity was reduced in the mimics and *METTL3*-WT groups relative to that in the mimics NC and *METTL3*-WT groups. Furthermore, transfection of mimics NC or mimics had almost no impact on luciferase activity in the *METTL3*-MUT group, demonstrating that *miR-let-7b* directly binds to *METTL3*. A *hsa_circ_0000523/miR-let-7b/METTL3* axis was thus identified in HCT116 cells.

Positive association between METTL3 expression and proliferation in HCT116 cells. As *METTL3* was the endpoint effector molecule for the *hsa_circ_0000523/miR-let-7b/METTL3* axis, it was important to elucidate the effects of *METTL3* expression on proliferation, apoptosis and invasion of HCT116 cells in the present study. Similarly, HCT116 cells with overexpression or knockdown of *METTL3* were generated by transfection of a *METTL3*-expressing pcDNA3.1 plasmid or a *METTL3*-specific siRNA oligo, respectively. The levels of *METTL3* mRNA were quantified using RT-qPCR and WB analysis. The results demonstrated that *METTL3* overexpression resulted in a >200-fold increase in *METTL3* transcript levels. The WB results were consistent with the RT-qPCR findings. Compared with the *METTL3*-con group, the *METTL3*-si group exhibited a >70% decrease in *METTL3* transcript levels (Fig. 2A).

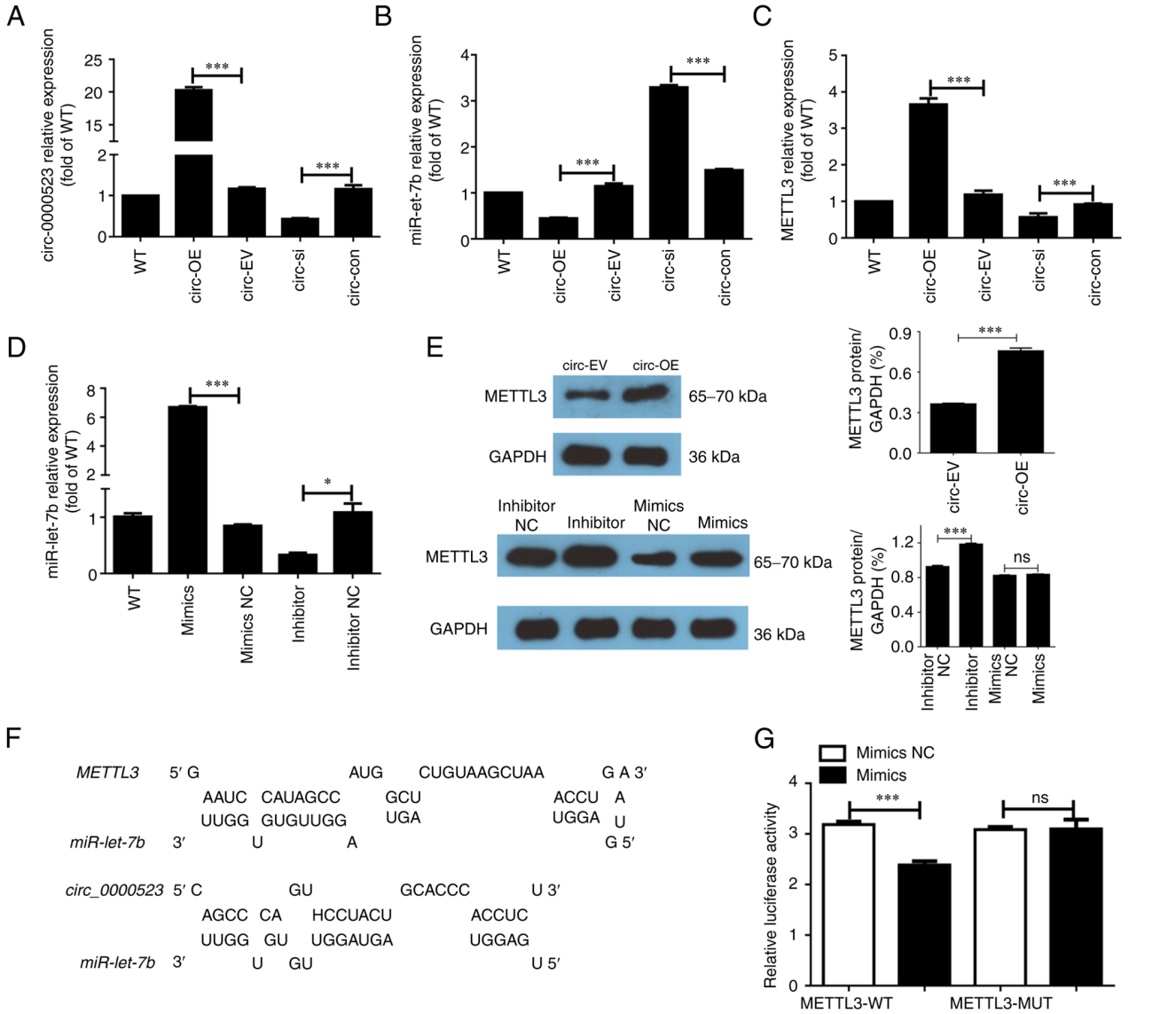

Figure 1. *hsa_circ_0000523* indirectly regulates *METTL3* expression by suppressing transcription of *miR-let-7b* in HCT116 cells. (A-C) HCT116 cells are untreated or transfected with *hsa_circ_0000523*-expression plasmid, empty pcDNA3.1 vector plasmid, *hsa_circ_0000523*-specific siRNA oligo or control siRNA oligo. At 48 h after transfection, HCT116 cells were harvested and transcriptional levels of (A) *hsa_circ_0000523*, (B) *miR-let-7b* and (C) *METTL3* are quantified by RT-qPCR. (D) RT-qPCR verifies the successful transfection of *miR-let-7b* mimics and inhibitor. (E) Protein levels of *METTL3* were measured using western blot analysis. (F) Schematic representation of *miR-let-7b* and predicted target site in *circ_0000523* and *METTL3*. (G) Interaction between *miR-let-7b* and *METTL3* was detected using a luciferase reporter assay. n=3 for each group. *P<0.05 and ***P<0.001. WT, untreated wild-type HCT116 cells; circ-OE, HCT116 cells with overexpression of hsa_*circ_0000523*; circ-EV, HCT116 cells transfected with empty vector; circ-si, HCT116 cells transfected with *hsa_circ_0000523*-specific siRNA oligo; circ-con, HCT116 cells transfected with negative control siRNA oligo; inhibitor, inhibitor-treated groups; inhibitor NC, the control of inhibitor-treated groups (PBS-treated groups); mimics, *miR-let-7b* overexpression groups; mimics NC, the control of mimics groups; *METTL3*, methyltransferase-like 3; RT-qPCR, reverse transcription-quantitative PCR; siRNA, small interfering RNA.

After transfection with plasmids or siRNA oligos, HCT116 cells were further cultured for 24, 48 or 72 h. Cell proliferation was measured at these time points using the CCK-8 assay. There were no significant differences in cell proliferation among the untreated WT, empty vector-transfected and negative control siRNA oligo-transfected HCT116 cells (Fig. 2B). Compared with the empty vector-transfected HCT116 cells (*METTL3*-EV group), HCT116 cells with ectopic expression of *METTL3* (*METTL3*-OE group) exhibited a significantly higher rate of proliferation at each time point. Cell proliferation was decreased in HCT116 cells with knockdown of *METTL3* compared with cells transfected with negative control siRNA oligos (Fig. 2B). Furthermore, the effects of *miR-let-7b* and *circ_0000523* on HCT116 cell proliferation were evaluated. Compared with the mimic NC groups, proliferation was obviously inhibited in the mimic groups. By contrast, cell viability was significantly promoted in inhibitor groups (Fig. 2C). As shown in Fig. 2D, overexpression of *circ_0000523* promoted HCT116 cell proliferation at all time points. Furthermore, *miR-let-7b* reversed the effects of *circ_0000523* overexpression on human HCT116 cell characteristics. Taken together, these results indicated that *hsa_circ_0000523* may regulate proliferation of CRC cells via *miR-let-7b*.

METTL3 regulates apoptosis in HCT116 cells. An important question was whether and how the expression of *METTL3*

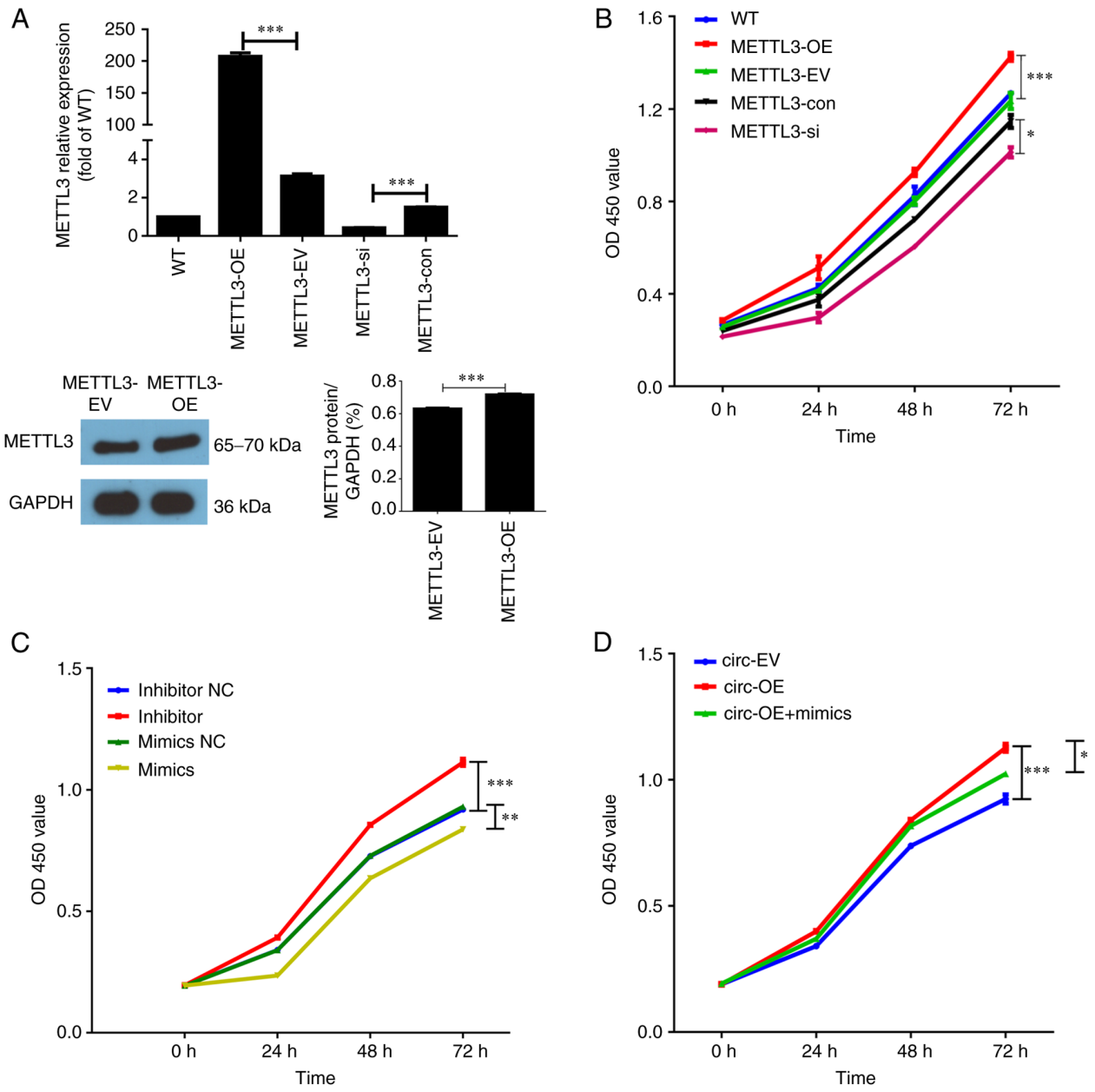

Figure 2. *METTL3*, *miR-let-7b* and *circ_0000523* regulate proliferation of HCT116 cells. (A) *METTL3* levels were quantified by reverse transcription-quantitative PCR or western blotting. (B-C) Cell Counting Kit-8 assays were performed to examine the role of (B) *METTL3* and (C) *miR-let-7b* in cell proliferation. (D) CCK-8 assays were used to detect the cell viability in each group. n=3 for each group. *P<0.05, **P<0.01 and ***P<0.001. WT, untreated wild-type HCT116 cells; *METTL3*-OE, HCT116 cells with overexpression of *METTL3*; *METTL3*-EV, HCT116 cells transfected with empty vector; *METTL3*-si, HCT116 cells transfected with *METTL3*-specific siRNA oligo; *METTL3*-con, HCT116 cells transfected with negative control siRNA oligo; inhibitor, inhibitor-treated group; inhibitor NC, the control of inhibitor-treated group (PBS-treated group); mimics, *miR-let-7b* overexpression groups; mimics NC, the control of mimics group; circ-OE, *circ_0000523* overexpression group; circ-EV, the control of circ-OE group; circ-OE + mimics, *circ_0000523* overexpressing vector and mimics co-transfected into HCT116 cells; *METTL3*, methyltransferase-like 3; siRNA, small interfering RNA; OD, optical density.

impacts apoptosis in HCT116 cells; therefore, this was evaluated using Annexin V and PI staining. There were no significant differences in apoptotic rates among the untreated WT, empty vector-transfected and negative control siRNA oligo-transfected HCT116 cells, all of which exhibited an apoptotic rate of ~15% (Fig. 3A and B). The rate of apoptosis was significantly decreased in HCT116 cells with ectopic expression of *METTL3* compared with HCT116 cells transfected with empty vector (12% vs. 15%, respectively). The rate of apoptosis was higher in HCT116 cells with knockdown of *METTL3* than in cells transfected with negative control siRNA oligos (20% vs. 15%, respectively; Fig. 3A and B). Therefore, a negative association between *METTL3* expression and the apoptotic rate was observed, which suggests that *METTL3* inhibits apoptosis in HCT116 cells. In addition, the effect of *circ_0000523* and *miR-let-7b* on HCT116 cell apoptosis was investigated by flow cytometry. Overexpression of *circ_0000523* significantly reduced apoptosis of CRC cells (Figs. 3C and S1A). Compared with that in the mimics NC group, the number of apoptotic cells was increased in the mimics group. By contrast, adding an inhibitor suppressed HCT116 cell apoptosis (Figs. 3D and S1B). As shown in

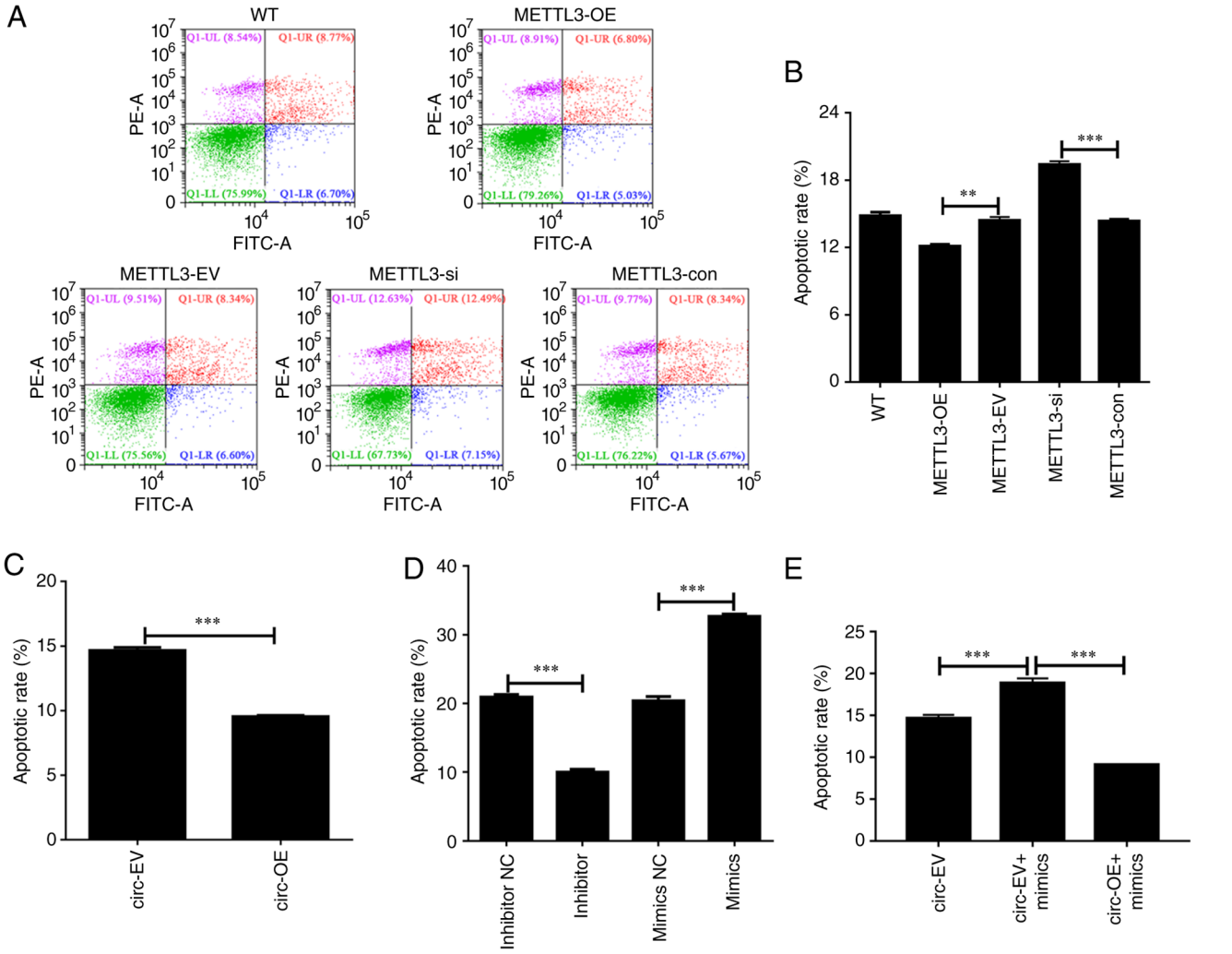

Figure 3. *METTL3*, *miR-let-7b* and *circ_0000523* mediate apoptosis of HCT116 cells. (A) Flow cytometry was used to detect apoptosis following knockdown or overexpression of *METTL3*. (B-D) Summarized data show the rate of apoptosis in HCT116 cells following interference with (B) *METTL3*, (C) *miR-let-7b* and (D) *circ_0000523*. (E) Representative flow cytometry apoptosis data for each group of CRC cells are shown. Annexin V-positive cells were considered to be apoptotic. n=3 for each group. **P<0.01 and ***P<0.001. WT, untreated wild-type HCT116 cells; *METTL3*-OE, HCT116 cells with overexpression of *METTL3*; *METTL3*-EV, HCT116 cells transfected with empty vector; *METTL3*-si, HCT116 cells transfected with *METTL3*-specific siRNA oligo; *METTL3*-OE, *METTL3* overexpression group; *METTL3*-con, the control of *METTL3*-OE group; inhibitor, inhibitor-treated group; inhibitor NC, the control of inhibitor-treated group (PBS-treated group); mimics, *miR-let-7b* overexpression groups; mimics NC, the control of mimics group; circ-OE, HCT116 cells with overexpression of *hsa_circ_0000523*; circ-EV, HCT116 cells transfected with empty vector; circ-EV + mimics, empty vector and mimics were co-transfected into HCT116 cells; circ-OE + mimics, *circ_0000523* overexpressing vector and mimics co-transfected into HCT116 cells; *METTL3*, methyltransferase-like 3; siRNA, small interfering RNA.

Figs. 3E and S1C, *circ_0000523* reversed the antitumor effects of *miR-let-7b* on human CRC cell line characteristics.

Higher METTL3 expression is associated with more aggressive tumor invasion in HCT116 cells. To explore the role of *METTL3* in regulating CRC metastasis, Transwell assays were performed to examine the invasion of HCT116 cells with various levels of *METTL3* expression. After plasmid (overexpression) or siRNA oligo (knockdown) transfection, the number of cells that had migrated to the surface of the lower chamber (filled with DMEM containing 10% FBS) was used as an index for the metastatic ability of HCT116 cells. As shown in Fig. 4A, a higher number of Giemsa-positive stained cells were observed in the group with *METTL3* overexpression compared with the group with *METTL3* knockdown.

Statistical analysis confirmed the positive association between *METTL3* expression and the invasion of HCT116 cells. There were no significant differences in invasion among the untreated WT, empty vector-transfected and negative control siRNA oligo-transfected HCT116 cells (Fig. 4A). Compared with empty vector-transfected HCT116 cells (*METTL3*-EV group), HCT116 cells with ectopic expression of *METTL3* (*METTL3*-OE group) exhibited significantly higher invasion. Consistently, invasion was decreased in HCT116 cells with *METTL3* knockdown compared with cells transfected with negative control siRNA oligos (Fig. 4A). These results suggest that higher expression of *METTL3* is associated with more aggressive tumor invasion in HCT116 cells. Next, it was examined whether *circ_0000523* and *miR-let-7p* mediate CRC cell invasion. Compared with those in the circ-EV group, cells in the lower chamber were increased by 43.2% in the circ-OE

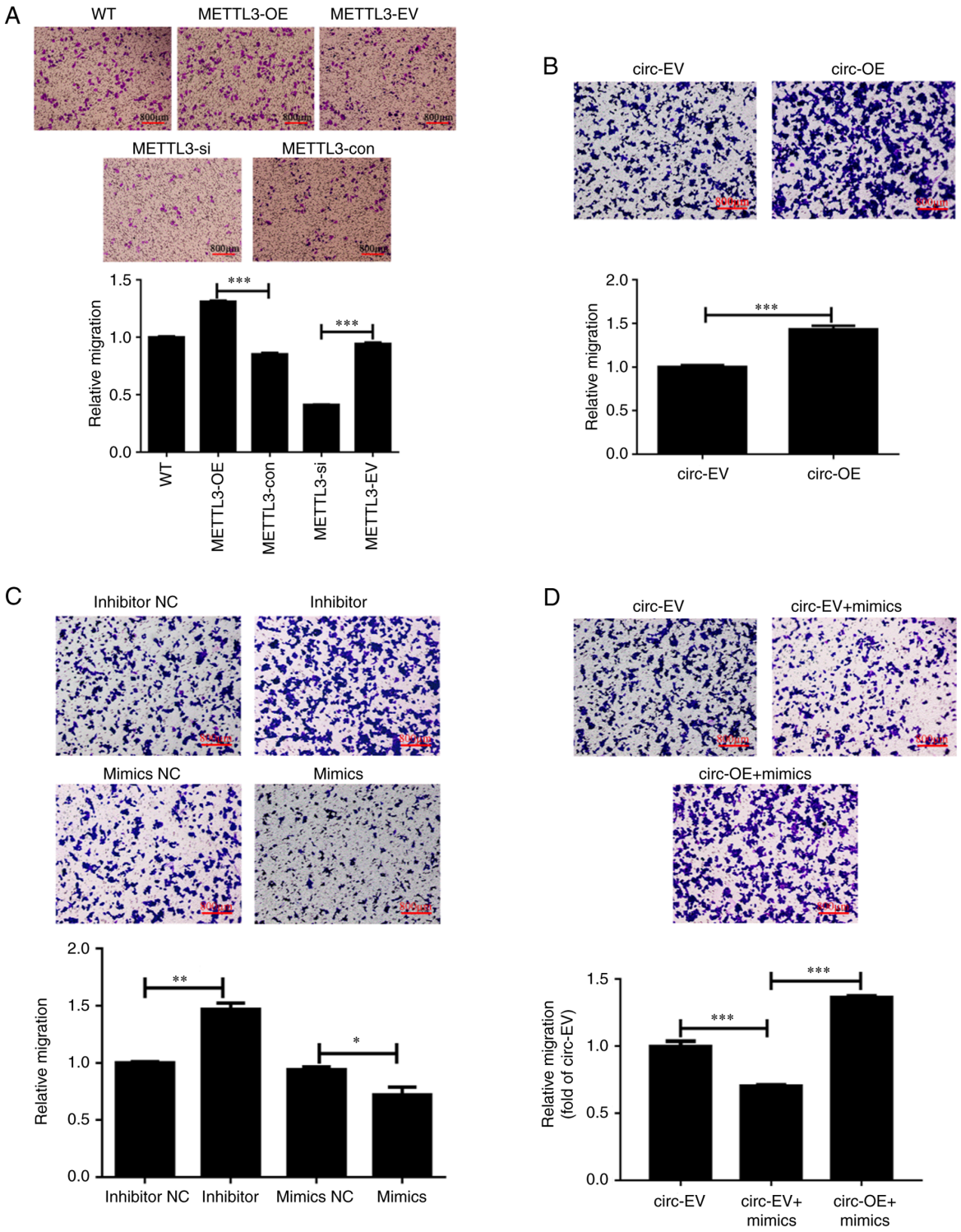

Figure 4. *METTL3*, *miR-let-7b* and *circ_0000523* mediate invasion of HCT116 cells. (A-C) Transwell assays reveal the invasion of HCT116 cells regulated by (A) *METTL3*, (B) *miR-let-7b* and (C) *circ_0000523*. (D) Transwell assays show the invasion abilities in each group. Scale bar, 800 μm. n=3 for each group; *P<0.05, **P<0.01 and ***P<0.001. WT, untreated wild-type HCT116 cells; *METTL3*-OE, HCT116 cells with overexpression of *METTL3*; *METTL3*-EV, HCT116 cells transfected with empty vector; *METTL3*-si, HCT116 cells transfected with *METTL3*-specific siRNA oligo; *METTL3*-con, the control of *METTL3*-si; inhibitor, inhibitor-treated groups; inhibitor NC, the control of inhibitor-treated groups; mimics, *miR-let-7b* overexpression groups; mimics NC, the control of mimics groups; circ-OE, HCT116 cells with overexpression of *hsa_circ_0000523*; circ-EV, HCT116 cells transfected with empty vector; circ-EV + mimics, empty vector and mimics co-transfected into HCT116 cells; circ-OE + mimics, *circ_0000523* overexpressing vector and mimics co-transfected into HCT116 cells; *METTL3*, methyltransferase-like 3; siRNA, small interfering RNA.

group, suggesting significant levels of invasion in CRC cells (Fig. 4B). The cell invasion of *miR-let-7b*-transfected cells (mimics group) obviously decreased compared with the control group (mimics NC group), while inhibitor treatment resulted in an obvious increase in CRC cell invasion ability (Fig. 4C). Furthermore, transfection of *miR-let-7b* mimics reduced the invasion of CRC cells; however, this was restored by *circ_0000523* overexpression (Fig. 4D).

Discussion

circRNAs modulate the expression of parental genes by regulating alternative splicing or transcription and acting as competitive sponges for endogenous RNA or miRNA (26). circRNAs may provide more comprehensive information on the key genes involved in oncogenesis and the development of numerous cancers (27,28). circRNAs are easily accessible and noninvasive biological markers for the early detection of CRC (29,30). However, few studies have reported on the specific functions of circRNAs in the tumorigenesis and pathogenesis of human CRC. In the present study, the expression patterns of *hsa_circ_0000523* and its parental gene *METTL3* were explored in the HCT116 human CRC cell line. The present results identified a potential *hsa_circ_0000523/miR-let-7b/METTL3* axis. The results of gain-of-function and loss-of-function assays demonstrated that expression of *METTL3* promoted cell proliferation and invasion and inhibited apoptosis in HCT116 cells. Rescue experiments were performed to confirm the regulatory effects of *hsa_circ_0000523* on *miR-let-7b*. It was found that *circ_0000523* reversed the antitumor effects of *miR-let-7b* on human CRC cell line characteristics.

Accumulating evidence has demonstrated the abnormal expression and important biological functions of circRNAs in CRC (12-14). circRNA plays various roles in CRC, including in proliferation, metastasis and apoptosis (6). Notably, most circRNAs previously identified by bioinformatic approaches have been found to be downregulated in CRC cell lines and clinical CRC tissues (17). Huang *et al* (31). demonstrated that the expression of circRNA itchy E3 ubiquitin ligase (*circ_ITCH*) was lower in CRC tissues compared with adjacent noncancerous tissues. *circ_ITCH* was found to sponge tumorigenic *miR-7* and *miR-20a*, which contribute to the malignancy of CRC (31). A positive association between transcription of *circ-ITCH* and the parental gene *ITCH* has been identified (31). Notably, expression of *circ-ITCH* was found to suppress proliferation in CRC cells (31). Similarly, Zhu *et al* (32) reported that *circ-BANP* was expressed in 35 CRC tissues, and knockdown of *circ-BANP* decreased the proliferation of CRC cells.

Indeed, there have been some studies reporting the regulatory role of circRNAs in tumourigenesis and progression of human CRC in previous years (33,34). Jin *et al* (35) found a deficiency in *hsa_circ_0000523* could activate the Wnt/β-catenin signaling pathway, which induced the development of CRC. To the best of our knowledge, the present study found for the first time that hsa_*circ_0000523* successfully promotes CRC via the *miR-let-7b/METTL3* axis.

In addition, the expression levels of *hsa_circ_0000523*, its potential target *miR-let-7b*, and its parental gene *METTL3* were evaluated in HCT116 cells. Similar to the expression patterns of *circ-ITCH* and *ITCH*, the transcript levels of *hsa_circ_0000523* were positively associated with mRNA levels of linear *METTL3* in HCT116 cells. Although the effects of *hsa_circ_0000523* expression on cell proliferation were not measured, the ability of *METTL3* expression to increase HCT116 cell proliferation suggests a similar proliferative role for *hsa_circ_0000523*. However, a previous report by Jin *et al* (35) demonstrated that *hsa_circ_0000523* exerted anti-proliferative effects and promoted apoptosis in two other human CRC cell lines (SW480 and SW620). Therefore, although *hsa_circ_0000523* can modulate *METTL3* expression by acting on *miR-let-7b*, additional studies will be necessary to determine whether the expression of *METTL3* can impact the transcription of *hsa_circ_0000523* in HCT116 cells.

circRNAs may regulate the proliferation of CRC by sequestering multiple miRNAs. For instance, circ-homeodomain interacting protein kinase 3 (circ-HIPK3) has been demonstrated to be upregulated in CRC tissue compared with normal tissue and regulates cell proliferation by sponging nine miRNAs with 18 potential binding sites (36). Specifically, circ-HIPK3 has been reported to bind to and inhibit the activity of miR-124, a tumor suppressor that is typically downregulated in CRC (37). Therefore, circRNAs may modulate the tumorigenic proliferation of CRC cells by diminishing the antitumor effects of certain tumor-suppressive miRNAs.

miR-let-7b, shown here to be a potential target of *hsa_circ_0000523*, is also a tumor suppressor in multiple cancers (38). Human *miR-let-7b* has been demonstrated to be downregulated in various cancers, and the induction of tumorigenesis was revealed to be inhibited in normal cells by ectopic expression of *miR-let-7b* (39,40). Human *miR-let-7* has been reported to inhibit cancer growth by targeting various oncogenes and inhibiting key regulators of several mitogenic pathways in cancer (38). These results point to a therapeutic potential for human *miR-let-7* in cancer treatment (38). Therefore, high levels of *hsa_circ_0000523* and low levels of *miR-let-7* may contribute to tumorigenesis in CRC.

On the other hand, circRNAs may regulate the proliferation of CRC by indirectly targeting oncogenes. *METTL3*, a target gene of *miR-let-7b,* was shown to promote growth, survival and invasion in human lung cancer (20). Furthermore, the oncogenic roles of *METTL3* have been demonstrated in numerous solid tumors and hematopoietic malignancies (41,42). For instance, it was found *METTL3* depletion inhibited tumorigenicity and sensitized lung cancer cells to bromodomain-containing protein 4 inhibition (42). To the best of our knowledge, the present study was the first report to describe the role of *METTL3* in CRC cells. *METTL3* expression in HCT116 cells was found to be positively associated with proliferation and cancer invasion and to be negatively associated with apoptosis. These findings suggest that *METTL3* functions as an oncogene in CRC, potentially by promoting the translation of other oncogenes. By contrast, *METTL3* has been found to be a tumor suppressor in renal cell carcinoma (43). *METTL3* has been demonstrated to promote cell proliferation, invasion and invasion in two human renal cell carcinoma cell lines (CAKI-1 and CAKI-2). These effects are mediated by modulation of the epithelial-to-mesenchymal transition and the PI3K-Akt-mTOR signaling pathway (43). The molecular mechanisms underlying the diverse roles of *METTL3* in renal cell carcinoma and CRC remain to be elucidated.

Through gain-of-function and siRNA oligo mediated loss-of-function experiments, a potential *hsa_circ_0000523/miR-let-7b/METTL3* axis, which contributed to tumorigenesis and pathogenesis in the HCT116 human CRC cell line, was identified. *METTL3* was demonstrated to promote proliferation and invasion and to inhibit apoptosis in HCT116 cells. The present study on the *hsa_circ_0000523/miR-let-7b/METTL3* axis may facilitate highly

sensitive diagnosis of CRC and improved prognosis prediction in patients following therapy.

Acknowledgements

Not applicable.

Funding

The present study was supported by grants from the Scientific Research Fund Project of Yunnan Education Department (grant no. 2019J1306). The funders had no role in study design, data collection, data analysis, decision to publish or preparation of the manuscript.

Availability of data and materials

The datasets used and/or analyzed during the current study are available from the corresponding author on reasonable request.

Authors' contributions

HL and YT designed and supervised the study. YW, BZ and LL were responsible for analyzing the data, writing the manuscript and revising it. YuZ, YoZ, LL and TS contributed to the statistical analysis of the data and text correction. All authors have read and approved the final manuscript. YW and BZ confirm the authenticity of all the raw data.

Ethics approval and consent to participate

Not applicable.

Patient consent for publication

Not applicable.

Competing interests

The authors declare that they have no competing interests.

References

1. Ferlay J, Soerjomataram I, Dikshit R, Eser S, Mathers C, Rebelo M, Parkin DM, Forman D and Bray F: Cancer incidence and mortality worldwide: Sources, methods and major patterns in GLOBOCAN 2012. Int J Cancer 136: E359-E386, 2015.
2. Marley AR and Nan H: Epidemiology of colorectal cancer. Int J Mol Epidemiol Genet 7: 105-114, 2016.
3. Torre LA, Bray F, Siegel RL, Ferlay J, Lortet-Tieulent J and Jemal A: Global cancer statistics, 2012. CA Cancer J Clin 65: 87-108, 2015.
4. Zhang Y, Chen Z and Li J: The current status of treatment for colorectal cancer in China: A systematic review. Medicine (Baltimore) 96: e8242, 2017.
5. Favoriti P, Carbone G, Greco M, Pirozzi F, Pirozzi RE and Corcione F: Worldwide burden of colorectal cancer: A review. Updates Surg 68: 7-11, 2016.
6. Fakih MG: Metastatic colorectal cancer: Current state and future directions. J Clin Oncol 33: 1809-1824, 2015.
7. Taborda MI, Ramirez S and Bernal G: Circular RNAs in colorectal cancer: Possible roles in regulation of cancer cells. World J Gastrointest Oncol 9: 62-69, 2017.
8. Salzman J: Circular RNA expression: Its potential regulation and function. Trends Genet 32: 309-316, 2016.
9. Meng X, Li X, Zhang P, Wang J, Zhou Y and Chen M: Circular RNA: An emerging key player in RNA world. Brief Bioinform 18: 547-557, 2017.
10. Memczak S, Jens M, Elefsinioti A, Torti F, Krueger J, Rybak A, Maier L, Mackowiak SD, Gregersen LH, Munschauer M, *et al*: Circular RNAs are a large class of animal RNAs with regulatory potency. Nature 495: 333-338, 2013.
11. Hansen TB, Jensen TI, Clausen BH, Bramsen JB, Finsen B, Damgaard CK and Kjems J: Natural RNA circles function as efficient microRNA sponges. Nature 495: 384-388, 2013.
12. Wang P and He X: Current research on circular RNAs associated with colorectal cancer. Scand J Gastroenterol 52: 1203-1210, 2017.
13. Zhang P, Zuo Z, Shang W, Wu A, Bi R, Wu J, Li S, Sun X and Jiang L: Identification of differentially expressed circular RNAs in human colorectal cancer. Tumor Biol: Mar 28, 2017 (Epub ahead of print).
14. Kristensen LS, Hansen TB, Venø MT and Kjems J: Circular RNAs in cancer: Opportunities and challenges in the field. Oncogene 37: 555-565, 2018.
15. Jiang W, Zhang X, Chu Q, Lu S, Zhou L, Lu X, Liu C, Mao L, Ye C, Timko MP, *et al*: The circular RNA profiles of colorectal tumor metastatic cells. Front Genet 9: 34, 2018.
16. Xu XW, Zheng BA, Hu ZM, Qian ZY, Huang CJ, Liu XQ and Wu WD: Circular RNA hsa_circ_000984 promotes colon cancer growth and metastasis by sponging miR-106b. Oncotarget 8: 91674-91683, 2017.
17. Bachmayr-Heyda A, Reiner AT, Auer K, Sukhbaatar N, Aust S, Bachleitner-Hofmann T, Mesteri I, Grunt TW, Zeillinger R and Pils D: Correlation of circular RNA abundance with proliferation-exemplified with colorectal and ovarian cancer, idiopathic lung fibrosis, and normal human tissues. Sci Rep 5: 8057, 2015.
18. Maity A and Das B: N6-methyladenosine modification in mRNA: Machinery, function and implications for health and diseases. FEBS J 283: 1607-1630, 2016.
19. Deng X, Su R, Weng H, Huang H, Li Z and Chen J: RNA N6-methyladenosine modification in cancers: Current status and perspectives. Cell Res 28: 507-517, 2018.
20. Lin S, Choe J, Du P, Triboulet R and Gregory RI: The m(6)A methyltransferase METTL3 promotes translation in human cancer cells. Mol Cell 62: 335-345, 2016.
21. Chen M, Wei L, Law CT, Tsang FH, Shen J, Cheng CL, Tsang LH, Ho DW, Chiu DK, Lee JM, *et al*: RNA N6-methyladenosine methyltransferase-like 3 promotes liver cancer progression through YTHDF2-dependent posttranscriptional silencing of SOCS2. Hepatology 67: 2254-2270, 2018.
22. Cai X, Wang X, Cao C, Gao Y, Zhang S, Yang Z, Liu Y, Zhang X, Zhang W and Ye L: HBXIP-elevated methyltransferase METTL3 promotes the progression of breast cancer via inhibiting tumor suppressor let-7g. Cancer Letters 415: 11-19, 2018.
23. Taketo K, Konno M, Asai A, Koseki J, Toratani M, Satoh T, Doki Y, Mori M, Ishii H and Ogawa K: The epitranscriptome m6A writer METTL3 promotes chemo- and radioresistance in pancreatic cancer cells. Int J Oncol 52: 621-629, 2018.
24. Brattain MG, Fine WD, Khaled FM, Thompson J and Brattain DE: Heterogeneity of malignant cells from a human colonic carcinoma. Cancer Res 41: 1751-1756, 1981.
25. Livak KJ and Schmittgen TD: Analysis of relative gene expression data using real-time quantitative PCR and the 2(-Delta Delta C(T)) method. Methods 25: 402-408, 2001.
26. Shao T, Pan YH and Xiong XD: Circular RNA: An important player with multiple facets to regulate its parental gene expression. Mol Ther Nucleic Acids 23: 369-376, 2020.
27. Huang X, Zhang W and Shao Z: Prognostic and diagnostic significance of circRNAs expression in lung cancer. J Cell Physiol 234: 18459-18465, 2019.
28. Ma Y, Zheng L, Gao Y, Zhang W, Zhang Q and Xu Y: A comprehensive overview of circRNAs: Emerging biomarkers and potential therapeutics in gynecological cancers. Front Cell Dev Biol 9: 709512, 2021.
29. Tian J, Xi X, Yu J, Huang Q, Ma R, Zhang X, Li H and Wang L: CircRNA hsa_circ_0004585 as a potential biomarker for colorectal cancer. Cancer Manag Res 11: 5413-5423, 2019.
30. Li RD, Guan M, Zhou Z, Dong SX and Liu Q: The role of circRNAs in the diagnosis of colorectal cancer: A meta-analysis. Front Med (Lausanne) 8: 766208, 2021.
31. Huang G, Zhu H, Shi Y, Wu W, Cai H and Chen X: cir-ITCH plays an inhibitory role in colorectal cancer by regulating the Wnt/β-catenin pathway. PLoS One 10: e0131225, 2015.
32. Zhu M, Xu Y, Chen Y and Yan F: Circular BANP, an upregulated circular RNA that modulates cell proliferation in colorectal cancer. Biomed Pharmacother 88: 138-144, 2017.

33. Peng K, Jiang P, Du Y, Zeng D, Zhao J, Li M, Xia C, Xie Z and Wu J: Oxidized low-density lipoprotein accelerates the injury of endothelial cells via circ-USP36/miR-98-5p/VCAM1 axis. IUBMB Life 73: 177-187, 2021.
34. Wu D, Jia H, Zhang Z and Li S: Circ-PRMT5 promotes breast cancer by the miR-509-3p/TCF7L2 axis activating the PI3K/AKT pathway. J Gene Med 23: e3300, 2021.
35. Jin Y, Yu LL, Zhang B, Liu CF and Chen Y: Circular RNA hsa_circ_0000523 regulates the proliferation and apoptosis of colorectal cancer cells as miRNA sponge. Braz J Med Biol Res 51: e7811, 2018.
36. Zheng Q, Bao C, Guo W, Li S, Chen J, Chen B, Luo Y, Lyu D, Li Y, Shi G, *et al*: Circular RNA profiling reveals an abundant circHIPK3 that regulates cell growth by sponging multiple miRNAs. Nat Commun 7: 11215, 2016.
37. Liu K, Yao H, Lei S, Xiong L, Qi H, Qian K, Liu J, Wang P and Zhao H: The miR-124-p63 feedback loop modulates colorectal cancer growth. Oncotarget 8: 29101-29115, 2017.
38. Barh D, Malhotra R, Ravi B and Sindhurani P: MicroRNA let-7: An emerging next-generation cancer therapeutic. Curr Oncol 17: 70-80, 2010.
39. Johnson CD, Esquela-Kerscher A, Stefani G, Byrom M, Kelnar K, Ovcharenko D, Wilson M, Wang X, Shelton J, Shingara J, *et al*: The let-7 microRNA represses cell proliferation pathways in human cells. Cancer Res 67: 7713-7722, 2007.
40. Kumar MS, Erkeland SJ, Pester RE, Chen CY, Ebert MS, Sharp PA and Jacks T: Suppression of non-small cell lung tumor development by the let-7 microRNA family. Proc Natl Acad Sci USA 105: 3903-3908, 2008.
41. Vu LP, Pickering BF, Cheng Y, Zaccara S, Nguyen D, Minuesa G, Chou T, Chow A, Saletore Y, MacKay M, *et al*: The N6-methyladenosine (m6A)-forming enzyme METTL3 controls myeloid differentiation of normal hematopoietic and leukemia cells. Nat Med 23: 1369, 2017.
42. Choe J, Lin S, Zhang W, Liu Q, Wang L, Ramirez-Moya J, Du P, Kim W, Tang S, Sliz P, *et al*: mRNA circularization by METTL3-eIF3h enhances translation and promotes oncogenesis. Nature 561: 556-560, 2018.
43. Li X, Tang J, Huang W, Wang F, Li P, Qin C, Qin Z, Zou Q, Wei J, Hua L, *et al*: The M6A methyltransferase METTL3: Acting as a tumor suppressor in renal cell carcinoma. Oncotarget 8: 96103-96116, 2017.